Advances in Nano Research, *Vol. 12, No. 1 (2022) 101-115*
https://doi.org/10.12989/anr.2022.12.1.101

Computational and mathematical simulation for the size-dependent dynamic behavior of the high-order FG nanotubes, including the porosity under the thermal effects

Xiaoping Huang[1], Huafeng Shan*[2], Weishen Chu[3] and Yongji Chen[4]

[1]*Guilin University of Technology, Guilin, Guangxi, China*
[2]*Keeson Technology Corporation Limited, Jiaxing 314000, Zhejiang, China*
[3]*Department of Mechanical Engineering, the University of Texas at Austin, TX 78712, Austin, USA*
[4]*Guangxi Mingxiang mechanical equipment testing Co., Ltd, Nanning, Guangxi, China*

(*Received August 5, 2021, Revised December 22, 2021, Accepted December 24, 2021*)

Abstract. Some researchers pointed out that the nonlocal cantilever models do not predict the dynamic softening behavior for nanostructures (including nanobeams) with clamped-free (CF) ends. In contrast, some indicate that the nonlocal cantilever models can capture the stiffness softening characteristics. There are substantial differences on this issue between them. The vibration analysis of porosity-dependent functionally graded nanoscale tubes with variable boundary conditions is investigated in this study. Using a modified power-law model, the tube's porosity-dependent material coefficients are graded in the radial direction. The theory of nonlocal strain gradients is used. Hamilton's principle is used to derive the size-dependent governing equations for simply-supported (S), clamped (C) and clamped-simply supported (CS). Following the solution of these equations by the extended differential quadrature technique, the effect of various factors on vibration issues was investigated further. It can be shown that these factors have a considerable effect on the vibration characteristics. It also can be found that our numerical results can capture the unexpected softening phenomena for cantilever tubes.
Keywords: free vibration; functionally graded porous tubes; higher-order theory; nonlocal strain gradient theory; various boundary conditions

1. Introduction

The application of nano-electro-mechanical systems (NEMS) has been widely used in many technologies, which caused many industrials, and many researchers have been focused on this field (Zhang *et al*. 2016, Wang *et al*. 2020a, 2022a, b Hu *et al*. 2021, Zhao *et al*. 2021a). The high-technology devices, including the thermal sensors, atomic force microscope (AFM), micro/- and nano-switches, vibration sensor, micro/- and nano actuators, etc., these wide applications lead to a wide range of researchers in all the world have worked on the development of the micro and nanosystems and related theories (Fazaeli *et al*. 2016, Ghazanfari *et al*. 2016, Habibi *et al*. 2016, 2018, Hosseini *et al*. 2018, Alipour *et al*. 2020, Cheshmeh *et al*. 2020, Ghabussi *et al*. 2020, Ghazanfari *et al*. 2020, Li *et al*. 2020a, 2020b, Liu *et al*. 2020a, b, Moayedi *et al*. 2020c, Shariati *et al*. 2020b, Shi *et al*. 2020, Wang *et al*. 2020b).

As it was explained, the investigation of small-scale devices and systems is one of the most popular issues in recent years, however, there are some problems in these topics, for example, experimental examinations proved that the classic theories are unable to handle and predict the behavior of the small-scale structures, so the high-order and non-classical theories are necessary to have a good view of the nanostructures. Eringen (1983) nonlocal theory is one of the most popular high-order and nonclassical theories that predicted the softening behavior due to the nonlocal impact on the nanostructures. On the other hand, Mindlin and Eshel (1968) suggested the strain gradient theory that predicted the hardening phenomenon due to the gradient strain parameter. However, the experimental tests confirmed that both hardening and softening phenomena could be happened in small-scale structures because of different conditions. To develop the previous non-classical theories, Lim *et al*. (2015) presented the nonlocal gradient strain theory, including both softening and hardening characteristics on the small-scale structures, in this theory, the deficiency of the primary theories is compensated. According to the development of the non-classical theories, in recent years, many researchers worked on small-scale structures such as the beam, tube, rod, plate, shell, and other applicable structures in order to investigate dynamic and static analysis (Hamidi *et al*. 2015, Allahkarami *et al*. 2017, Ehyaei *et al*. 2017a, Akbaş 2018a, b, Arefi and Zenkour 2018, Aydogdu *et al*. 2018, Bensaid *et al*. 2018, Navi *et al*. 2019, Ebrahimi *et al*. 2020, Gafour *et al*. 2020, Matouk *et al*. 2020).

Some studies show that (Aranda-Ruiz *et al*. 2012, Sadri *et al*. 2016, Azimi *et al*. 2018) the fundamental frequency of nanobeams with clamped-free ends have a unique behavior, and shown that the nonlocal cantilever models can predict the stiffness hardening behavior, while some others (Eltaher *et al*. 2014, Xu *et al*. 2016, 2017) indicates that the nonlocal

*Corresponding author, Mr.,
E-mail: victor8068@163.com

ISSN: 2287-237X (Print), 2287-2388 (Online)

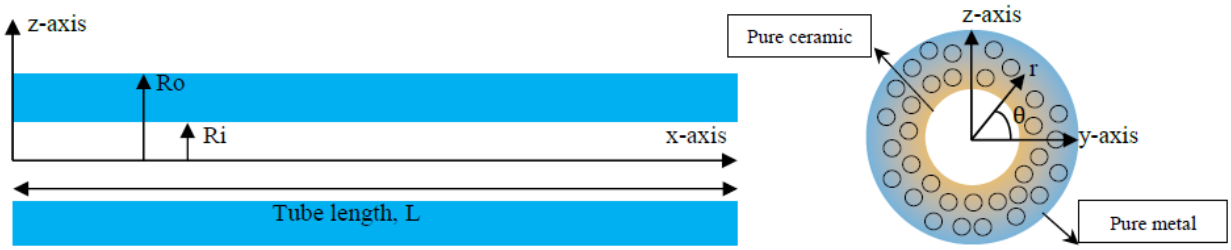

Fig. 1 A nanotube's geometry and coordinated system (She *et al*. 2018a)

cantilever models can capture the stiffness softening characteristics. It is clear that there are substantial differences on this issue between them, it is this fact that prompt us to undertake the following study. The current article employs the generalized differential quadrature technique to investigate functionally graded porous nanoscaled tubes with four distinct boundary conditions and draws some significant results.

2. Mathematic and structural equations

Fig. 1 presents the porosity-dependent functionally graded tube that the porosity void is dispersed in the radial direction. The tube length is denoted with 'L', the internal radius is 'R_i', and the external radius is 'R_o'. Also, the materials are gradually changed in the radial direction between the ceramic and metal phases. The inner tube surface is pure ceramic, and the outer tube surface is pure metal.

In addition, the material properties (including Young's modulus E, mass density ρ and thermal expansion coefficient α) of the nanotube with porosity vary along the radial direction (r- direction), as

$$\begin{aligned}
&E(r,T)=\left(E_c(T)-E_m(T)\right)\left(\frac{r-R_i}{R_0-R_i}\right)^n+E_m(T)\\
&-\beta\cos\left(\frac{\pi}{2}\frac{r-R_i}{R_0-R_i}\right)\left[\left(E_c(T)-E_m(T)\right)\left(\frac{r-R_i}{R_0-R_i}\right)^n+E_m(T)\right]\\
&\alpha(r,T)=\left(\alpha_c(T)-\alpha_m(T)\right)\left(\frac{r-R_i}{R_0-R_i}\right)^n+\alpha_m(T)\\
&-\beta\cos\left(\frac{\pi}{2}\frac{r-R_i}{R_0-R_i}\right)\left[\left(\alpha_c(T)-\alpha_m(T)\right)\left(\frac{r-R_i}{R_0-R_i}\right)^n+\alpha_m(T)\right]\\
&\rho(r,T)=\left(\rho_c(T)-\rho_m(T)\right)\left(\frac{r-R_i}{R_0-R_i}\right)^n+\rho_m(T)\\
&-\beta\cos\left(\frac{\pi}{2}\frac{r-R_i}{R_0-R_i}\right)\left[\left(\rho_c(T)-\rho_m(T)\right)\left(\frac{r-R_i}{R_0-R_i}\right)^n+\rho_m(T)\right]
\end{aligned}\tag{1}$$

In this equation, c and m stand for the ceramic and metal. Where 'r' is the radial variation, FG parameter is 'n', the porous parameter is 'β', and 'T' is the temperature that is applied in the mechanical properties of material on the basis of the Touloukian and Ho (1970) relation which are listed in Table 1.

Based on Zhang and Fu's tube model (Lim *et al*. 2015), The displacement along the x, y, and z axes may be expressed as

$$\begin{aligned}
&u_1(x,y,z,t)=u+g(y,z)\left[\frac{\partial w(x,t)}{\partial x}+\psi(x,t)\right]-z\frac{\partial w(x,t)}{\partial x}\\
&u_2=0,u_3(x,y,z,t)=w(x,t)
\end{aligned}\tag{2}$$

where

$$g(y,z)=z\times\left[\frac{\left(R_0{}^2R_i{}^2r^{-2}-\frac{r^2}{3}\right)}{\left(R_0{}^2+R_i{}^2\right)}+1\right]\tag{3}$$

where 'u' denotes axial displacement, 'w' denotes transverse displacement, 'ψ' denotes rotation, and 't' denotes time. It should be noted that 'g = z' for the Timoshenko beam model. We may calculate the strains using Eq. (2).

$$\begin{aligned}
&\varepsilon_{xx}=\frac{\partial u_1}{\partial x}=\frac{\partial u}{\partial x}+\frac{1}{2}\left(\frac{\partial w}{\partial x}\right)^2-z\frac{\partial^2 w}{\partial x^2}\\
&+g(y,z)\left(\frac{\partial^2 w}{\partial x^2}+\frac{\partial\psi}{\partial x}\right),\quad \varepsilon_T=\alpha\Delta T,\\
&\varepsilon_{xy}=\frac{1}{2}\left(\frac{\partial u_1}{\partial y}+\frac{\partial u_2}{\partial x}\right)=\frac{1}{2}\frac{\partial g(y,z)}{\partial y}\left(\frac{\partial w}{\partial x}+\psi\right)\\
&\varepsilon_{xz}=\frac{1}{2}\left(\frac{\partial u_1}{\partial z}+\frac{\partial u_3}{\partial x}\right)=\frac{1}{2}\frac{\partial g(y,z)}{\partial z}\left(\frac{\partial w}{\partial x}+\psi\right)
\end{aligned}\tag{4}$$

Then, we can obtain the stresses, as

$$\begin{aligned}
&\sigma_{xx}=E\varepsilon_{xx}-E\varepsilon_T,\sigma_{xy}=G\varepsilon_{xy},\\
&\sigma_{xz}=G\varepsilon_{xy},G=\frac{E}{2(1+\nu)}
\end{aligned}\tag{5}$$

The Hamilton principle is used to generate and develop the governing equation as well as boundary conditions.

$$\int_{t_1}^{t_2}\delta\Pi dt=\int_{t_1}^{t_2}(\delta S-\delta K)dt=0\tag{6}$$

where 'δS' is the virtual strain energy, which may be calculated as

$$\begin{aligned}
&\delta S=\iiint\delta\varepsilon dv=\\
&=-\int_0^L\frac{\partial}{\partial x}\left(A_{11}\frac{\partial u}{\partial x}\right)dx\,\delta(u)+A_{11}\frac{\partial u}{\partial x}\Big|_0^L\delta(u)\\
&+\int_0^L\frac{\partial^2}{\partial x^2}\left(D_{11}\frac{\partial^2 w}{\partial x^2}\right)dx\,\delta(w)+D_{11}\frac{\partial^2 w}{\partial x^2}\Big|_0^L\delta\left(\frac{\partial w}{\partial x}\right)\\
&-\frac{\partial}{\partial x}\left(D_{11}\frac{\partial^2 w}{\partial x^2}\right)\Big|_0^L\delta(w)+\int_0^L\frac{\partial^2}{\partial x^2}\left(H_{11}\frac{\partial^2 w}{\partial x^2}\right)dx\,\delta(w)\\
&+H_{11}\frac{\partial^2 w}{\partial x^2}\Big|_0^L\delta\left(\frac{\partial w}{\partial x}\right)-\frac{\partial}{\partial x}\left(H_{11}\frac{\partial^2 w}{\partial x^2}\right)\Big|_0^L\delta(w)\\
&-\int_0^L\frac{\partial}{\partial x}\left(H_{11}\frac{\partial\psi}{\partial x}\right)dx\,\delta(\psi)+A_{11}\frac{\partial\psi}{\partial x}\Big|_0^L\delta(\psi)\\
&-\int_0^L\frac{\partial}{\partial x}\left(H_{11}\frac{\partial^2 w}{\partial x^2}\right)dx\,\delta(\psi)+H_{11}\frac{\partial^2 w}{\partial x^2}\Big|_0^L\delta(\psi)\\
&+\int_0^L\frac{\partial^2}{\partial x^2}\left(H_{11}\frac{\partial\psi}{\partial x}\right)dx\,\delta(w)+H_{11}\frac{\partial\psi}{\partial x}\Big|_0^L\delta\left(\frac{\partial w}{\partial x}\right)
\end{aligned}\tag{7}$$

$$
\begin{aligned}
&-\frac{\partial}{\partial x}\left(H_{11}\frac{\partial\psi}{\partial x}\right)\Big|_0^L\delta(w)-2\int_0^L\frac{\partial^2}{\partial x^2}\left(E_{11}\frac{\partial^2 w}{\partial x^2}\right)dx\,\delta(w)\\
&-2\,E_{11}\frac{\partial^2 w}{\partial x^2}\Big|_0^L\delta\left(\frac{\partial w}{\partial x}\right)+2\frac{\partial}{\partial x}\left(E_{11}\frac{\partial^2 w}{\partial x^2}\right)\Big|_0^L\delta(w)\\
&+\int_0^L\frac{\partial}{\partial x}\left(E_{11}\frac{\partial^2 w}{\partial x^2}\right)dx\,\delta(\psi)-E_{11}\frac{\partial^2 w}{\partial x^2}\Big|_0^L\delta(\psi)\\
&-\int_0^L\frac{\partial^2}{\partial x^2}\left(E_{11}\frac{\partial\psi}{\partial x}\right)dx\,\delta(w)-E_{11}\frac{\partial\psi}{\partial x}\Big|_0^L\delta\left(\frac{\partial w}{\partial x}\right)\\
&+\frac{\partial}{\partial x}\left(E_{11}\frac{\partial\psi}{\partial x}\right)\Big|_0^L\delta(w)+\int_0^L\frac{\partial}{\partial x}(N_T)dx\,\delta(u)\\
&-N_T|_0^L\delta(u)+\int_0^L\frac{\partial}{\partial x}\left(N_T\frac{\partial w}{\partial x}\right)dx\,\delta(w)\\
&-N_T\frac{\partial w}{\partial x}\Big|_0^L\delta(w)-\int_0^L\frac{\partial}{\partial x}\left(B_{11}\frac{\partial w}{\partial x}\right)dx\,\delta(w)\\
&+B_{11}\frac{\partial w}{\partial x}\Big|_0^L\delta(w)+\int_0^L B_{11}\psi\delta(\psi)+B_{11}\frac{\partial w}{\partial x}\delta(\psi)\,dx\\
&-\int_0^L\frac{\partial}{\partial x}\big(B_{11}(\psi)\big)dx\,\delta(w)+B_{11}\psi|_0^L\delta(w)
\end{aligned}
$$

In which

$$
\begin{aligned}
(A_{11},D_{11},E_{11},H_{11})&=\int_A E_f(r,T)\,(1,z^2,zg,g^2)dA,\\
B_{11}&=\int_A G_f(r,T)\left[\left(\frac{\partial g}{\partial y}\right)^2+\left(\frac{\partial g}{\partial z}\right)^2\right]dA
\end{aligned}
\tag{8a}
$$

$$
N_T=\iint E(r,T)\alpha(r,T)\Delta T\,dA \tag{8b}
$$

The variation of kinetic energy can be derived as

$$
\begin{aligned}
\delta K&=\int_\Omega\rho(T)\left[\frac{\partial u_1}{\partial t}\delta\left(\frac{\partial u_1}{\partial t}\right)+\frac{\partial u_3}{\partial t}\delta\left(\frac{\partial u_3}{\partial t}\right)\right]d\Omega\\
&=\int_0^L\left\{\int_A\rho(T)\left[\frac{\partial u_1}{\partial t}\delta\left(\frac{\partial u_1}{\partial t}\right)+\frac{\partial u_3}{\partial t}\delta\left(\frac{\partial u_3}{\partial t}\right)\right]dA\right\}dx\\
&=\int_0^L\Big\{m_0(T)\left[\frac{\partial u}{\partial t}\delta\left(\frac{\partial u}{\partial t}\right)+\frac{\partial w}{\partial t}\delta\left(\frac{\partial w}{\partial t}\right)\right]\\
&+m_1(T)\frac{\partial^2 w}{\partial x\partial t}\delta\left(\frac{\partial^2 w}{\partial x\partial t}\right)\\
&+m_2(T)\left[-\frac{\partial\psi}{\partial t}\delta\left(\frac{\partial^2 w}{\partial x\partial t}\right)-2\frac{\partial^2 w}{\partial x\partial t}\delta\left(\frac{\partial^2 w}{\partial x\partial t}\right)-\frac{\partial^2 w}{\partial x\partial t}\delta\left(\frac{\partial\psi}{\partial t}\right)\right]\\
&+m_3(T)\left[\begin{aligned}&\frac{\partial^2 w}{\partial x\partial t}\delta\left(\frac{\partial^2 w}{\partial x\partial t}\right)+\frac{\partial\psi}{\partial t}\delta\left(\frac{\partial^2 w}{\partial x\partial t}\right)\\&+\frac{\partial^2 w}{\partial x\partial t}\delta\left(\frac{\partial\psi}{\partial t}\right)+\left(\frac{\partial\psi}{\partial t}\right)\delta\left(\frac{\partial\psi}{\partial t}\right)\end{aligned}\right]\Big\}dx
\end{aligned}
\tag{9}
$$

In which

$$
(m_0,m_1,m_2,m_3)=\int_A\rho_f(T,r)\,(1,z^2,zg,g^2)dA \tag{10}
$$

The Euler-Lagrangian equations are obtained by substituting Eqs. (7) and (9) into Eq. (6)).

$$
\begin{aligned}
&\delta u:\frac{\partial N}{\partial x}=m_0(T)\frac{\partial^2 u}{\partial t^2}\\
&\delta\varphi:\frac{\partial P}{\partial x}-Q\\
&=-m_2(T)\frac{\partial^3 w}{\partial x\partial t^2}+m_3(T)\left(\frac{\partial^3 w}{\partial x\partial t^2}+\frac{\partial^2\psi}{\partial t^2}\right)\\
&\delta w:\frac{\partial^2 P}{\partial x^2}-\frac{\partial^2 M}{\partial x^2}-\frac{\partial Q}{\partial x}=q-N_T\frac{\partial^2 w}{\partial x^2}
\end{aligned}
\tag{11}
$$

$$
\begin{aligned}
&-m_0(T)\frac{\partial^2 w}{\partial t^2}+m_1(T)\frac{\partial^4 w}{\partial x^2\partial t^2}\\
&-m_2(T)\left(2\frac{\partial^4 w}{\partial x^2\partial t^2}+\frac{\partial^3\psi}{\partial x\partial t^2}\right)\\
&+m_3(T)\left(\frac{\partial^4 w}{\partial x^2\partial t^2}+\frac{\partial^3\psi}{\partial x\partial t^2}\right)
\end{aligned}
$$

where

$$
N=A_{11}\frac{\partial u}{\partial x} \tag{12a}
$$

$$
P=H_{11}\left(\frac{\partial^2 w}{\partial x^2}+\frac{\partial\psi}{\partial x}\right)-E_{11}\frac{\partial^2 w}{\partial x^2} \tag{12b}
$$

$$
M=E_{11}\left(\frac{\partial^2 w}{\partial x^2}+\frac{\partial\psi}{\partial x}\right)-D_{11}\frac{\partial^2 w}{\partial x^2} \tag{12c}
$$

$$
Q=B_{11}\left(\frac{\partial w}{\partial x}+\psi\right) \tag{12d}
$$

Moreover, the derived equations of boundary conditions are as follows:

$$
\begin{aligned}
&u=0 or N_{xx}|_0^L-N_T|_0^L=0\\
&w=0 or\frac{\partial M}{\partial x}-\frac{\partial P}{\partial x}+Q-N_T\frac{\partial w}{\partial x}\Big|_0^L=0\\
&\psi=0 or P|_0^L=0\\
&\frac{\partial w}{\partial x}=0 or M-P|_0^L=0
\end{aligned}
\tag{13}
$$

3. Impact of nonlocal strain gradient theory

Lim *et al*. (2015) presented the nonlocal strain gradient theory (NSGT), which is a mixture of Eringen (1983) nonlocal stress theory and Aifantis (1992) and Mindlin (1965) strain gradient theories. This idea incorporates two distinct scaling effects. The nonlocal strain gradient theory makes the following assumptions about the total stress tensor 't_{xx}':

$$
[1-(ea)^2\nabla^2]t_{xx}=E(1-l^2\nabla^2)\varepsilon_{xx} \tag{14}
$$

According to the NGST, the stress resultants (Eq. (12)) can be rewriting as

$$
\begin{aligned}
N&=(ea)^2\frac{\partial^2 N}{\partial x^2}+A_{11}(T)\left(1-l^2\frac{\partial^2}{\partial x^2}\right)\left(\frac{\partial u}{\partial x}-N_T(T)\right)\\
M&=(ea)^2\frac{\partial^2 M}{\partial x^2}+\left(1-l^2\frac{d^2}{dx^2}\right)\left[-D_{11}(T)\frac{\partial^2 w}{\partial x^2}\right.\\
&\qquad\left.+E_{11}(T)\left(\frac{\partial^2 w}{\partial x^2}+\frac{\partial\psi}{\partial x}\right)\right]\\
P&=(ea)^2\frac{\partial^2 P}{\partial x^2}+\left(1-l^2\frac{\partial^2}{\partial x^2}\right)\left[-E_{11}(T)\frac{\partial^2 w}{\partial x^2}\right.\\
&\qquad\left.+H_{11}(T)\left(\frac{\partial^2 w}{\partial x^2}+\frac{\partial\psi}{\partial x}\right)\right]\\
Q&=(ea)^2\frac{\partial^2 Q}{\partial x^2}+\left(1-l^2\frac{\partial^2}{\partial x^2}\right)B_{11}(T)\left(\psi+\frac{\partial w}{\partial x}\right)
\end{aligned}
\tag{15}
$$

Based on Hamiltonian variational principle (Moayedi *et al*. 2020a, b, Oyarhossein *et al*. 2020, Shariati *et al*. 2020a,

Zhou *et al*. 2020, Dai *et al*. 2021b, Guo *et al*. 2021a, b, He *et al*. 2021, Huang *et al*. 2021a, Huo *et al*. 2021, Liu *et al*. 2021b, Peng *et al*. 2021, Shao *et al*. 2021, Zhang *et al*. 2021a, b, c) and NSGT (Lim *et al*. 2015a), the motion equations can be derived as

$$\begin{aligned}&\delta u: A_{11}(T)\frac{\partial^2 u}{\partial x^2}-l^2\left(A_{11}(T)\frac{\partial^4 u}{\partial x^4}\right)\\&=m_0(T)\frac{\partial^2 u}{\partial t^2}-(e_0a^2)\left(m_0(T)\frac{\partial^4 u}{\partial x^2\partial t^2}\right)\end{aligned}\tag{16a}$$

$$\begin{aligned}&\psi:\ EE(T)\frac{\partial^3 w}{\partial x^3}+H_{11}(T)\frac{\partial^2\psi}{\partial x^2}-B_{11}(T)\left(\frac{\partial w}{\partial x}+\psi\right)\\&-l^2\begin{bmatrix}EE(T)\dfrac{\partial^5 w}{\partial x^5}+H_{11}(T)\dfrac{\partial^4\psi}{\partial x^4}\\-B_{11}(T)\dfrac{\partial^3 w}{\partial x^3}-B_{11}(T)\dfrac{\partial^2\psi}{\partial x^2}\end{bmatrix}\\&=I_2(T)\frac{\partial^3 w}{\partial t^2\partial x}+m_3(T)\frac{\partial^2\psi}{\partial t^2}\\&-(e_0a^2)\left[I_2(T)\frac{\partial^5 w}{\partial x^3\partial t^2}+m_3(T)\frac{\partial^4\psi}{\partial x^2\partial t^2}\right]\end{aligned}\tag{16b}$$

$$\begin{aligned}&E(T)\frac{\partial^4 w}{\partial x^4}+EE(T)\frac{\partial^3\psi}{\partial x^3}-B_{11}(T)\left(\frac{\partial^2 w}{\partial x^2}+\frac{\partial\psi}{\partial x}\right)\\&+N^T(T)\frac{\partial^2 w}{\partial x^2}-l^2\begin{bmatrix}E(T)\dfrac{\partial^6 w}{\partial x^6}+EE(T)\dfrac{\partial^5\psi}{\partial x^5}\\-B_{11}(T)\dfrac{\partial^4 w}{\partial x^4}-B_{11}(T)\dfrac{\partial^3\psi}{\partial x^3}\end{bmatrix}\\&-(e_0a^2)N^T(T)\frac{\partial^4 w}{\partial x^4}=I_1(T)\frac{\partial^4 w}{\partial t^2\partial x^2}\\&-m_0(T)\frac{\partial^2 w}{\partial t^2}+I_2(T)\frac{\partial^3\psi}{\partial x\partial t^2}\\&-(e_0a^2)\begin{bmatrix}I_1(T)\dfrac{\partial^6 w}{\partial x^4\partial t^2}-m_0(T)\dfrac{\partial^4 w}{\partial x^2\partial t^2}\\+I_2(T)\dfrac{\partial^5\psi}{\partial x^3\partial t^2}\end{bmatrix}\end{aligned}\tag{16c}$$

In which

$$\begin{aligned}&E(T)=H_{11}(T)+D_{11}(T)-2E_{11}(T)\\&EE(T)=H_{11}(T)-E_{11}(T)\\&I_1(T)=m_3(T)+m_1(T)-2m_2(T)\\&I_2(T)=m_3(T)-m_2(T)\end{aligned}\tag{17}$$

4. Approach to problem-solving

An algorithm known as the GDQM (Dai *et al*. 2021a, Ebrahimi *et al*. 2021, Hashemi *et al*. 2021, Hou *et al*. 2021, Huang *et al*. 2021b, c, Jiao *et al*. 2021, Liu *et al*. 2021a, c, Ma *et al*. 2021, Moradi *et al*. 2021, Najaafi *et al*. 2021, Shariati *et al*. 2021, Wu and Habibi 2021, Xu *et al*. 2021, Zhao *et al*. 2021b, Yu *et al*. 2022) is used to solve Equation (16). The r-th order derivative of the function '$f(x_i)$' is as follows:

$$\left.\frac{\partial^r f(x)}{\partial x^r}\right|_{x=x_P}=\sum_{j=1}^{k}C_{ij}^{(r)}f(x_i)\tag{18}$$

k is the number of grid points along x direction and C_{ij} is:

$$\begin{aligned}&C_{ij}^{(1)}=\frac{M(x_i)}{(x_i-x_j)M(x_j)},i,j=1,2,\dots,k and\ i\neq j\\&C_{ij}^{(1)}=-\sum_{j=1,i\neq j}^{n}C_{ij}^{(1)},i=j\end{aligned}\tag{19}$$

In which

$$M(x_i)=\prod_{j=1,j\neq i}^{k}(x_i-x_j)\tag{20a}$$

$$\begin{aligned}&C_{ij}^{(r)}=r\left[C_{ij}^{(r-1)}C_{ij}^{(1)}-\frac{C_{ij}^{(r-1)}}{(x_i-x_j)}\right],i,j\\&=1,2,\dots,k,i\neq j\quad and 2\le r\le k-1\\&C_{ii}^{(r)}=-\sum_{j=1,i\neq j}^{n}C_{ij}^{(r)},i,j\\&=1,2,\dots,k\ and\ 1\le r\le k-1\end{aligned}\tag{20b}$$

The Chebyshev-Gauss-Lobatto method is used to distribute mesh points (Azimi *et al*. 2016, Ebrahimi and Shafiei 2016, Ghadiri *et al*. 2016a, b, c, d, Ghadiri and Shafiei 2016a, b, c, Shafiei *et al*. 2016a, b, c, d, e, f, g).

$$x_i=\frac{L}{2}\left(1-cos\left(\frac{(i-1)}{(N-1)}\pi\right)\right)i=1,2,3,\dots,k\tag{21}$$

For the FG nanotube boundary conditions and vibration equations, two matrixes must be combined. It is therefore possible to compute the stiffness matrixes

$$\{[K]-\omega^2[M]\}\{\lambda\}=0\tag{22}$$

Last but not least, we apply weighting factors Eq. (20) into Eq. (16) to arrive at the following result:

$$\begin{aligned}&A_{11}\sum_{s=1}^{n}C_{rs}{}^{(2)}u_s-l^2\left(A_{11}\sum_{s=1}^{n}C_{rs}{}^{(4)}u_s\right)\\&=m_0\sum_{s=1}^{n}C_{rs}{}^{(2)}u_s-(e_0a^2)m_0\sum_{s=1}^{n}C_{rs}{}^{(4)}u_s\end{aligned}\tag{23a}$$

$$\begin{aligned}&EE\sum_{s=1}^{n}C_{rs}{}^{(3)}w_s+H_{11}\sum_{s=1}^{n}C_{rs}{}^{(2)}\psi_s\\&-B_{11}\left(\sum_{s=1}^{n}C_{rs}{}^{(1)}w_s+\psi_s\right)\\&-l^2\begin{bmatrix}EE\sum_{s=1}^{n}C_{rs}{}^{(5)}w_s+H_{11}\sum_{s=1}^{n}C_{rs}{}^{(4)}\psi_s\\-B_{11}\left(\sum_{s=1}^{n}C_{rs}{}^{(3)}w_s+\sum_{s=1}^{n}C_{rs}{}^{(2)}\psi_s\right)\end{bmatrix}\\&=\omega^2\begin{bmatrix}I_2\sum_{s=1}^{n}C_{rs}{}^{(1)}w_s+m_3\psi_s\\-(e_0a^2)\left(I_2\sum_{s=1}^{n}C_{rs}{}^{(3)}w_s+m_3\sum_{s=1}^{n}C_{rs}{}^{(2)}\psi_s\right)\end{bmatrix}\end{aligned}\tag{23b}$$

$$
\begin{aligned}
&E\sum_{s=1}^{n} C_{rs}{}^{(4)} w_s + EE\sum_{s=1}^{n} C_{rs}{}^{(3)} \psi_s \\
&-B_{11}\left(\sum_{s=1}^{n} C_{rs}{}^{(2)} w_s + \sum_{s=1}^{n} C_{rs}{}^{(1)} \psi_s\right) + N^T \sum_{s=1}^{n} C_{rs}{}^{(2)} w_s \\
&-l^2\begin{bmatrix} E\sum_{s=1}^{n} C_{rs}{}^{(6)} w_s + EE\sum_{s=1}^{n} C_{rs}{}^{(5)} \psi_s \\ -B_{11}\left(\sum_{s=1}^{n} C_{rs}{}^{(4)} w_s + \sum_{s=1}^{n} C_{rs}{}^{(3)} \psi_s\right) \end{bmatrix} \\
&-(e_0a^2)N^T \sum_{s=1}^{n} C_{rs}{}^{(4)} w_s \\
&= \omega^2 \begin{bmatrix} I_1\sum_{s=1}^{n} C_{rs}{}^{(2)} w_s - m_0 w_s + I_2\sum_{s=1}^{n} C_{rs}{}^{(1)} \psi_s \\ -(e_0a^2)\left(I_1\sum_{s=1}^{n} C_{rs}{}^{(4)} w_s - m_0\sum_{s=1}^{n} C_{rs}{}^{(2)} w_s + I_2\sum_{s=1}^{n} C_{rs}{}^{(3)} \psi_s\right) \end{bmatrix}
\end{aligned}
\tag{23c}
$$

Considering the different boundary conditions, the fundamental vibration of FG nanotubes can be calculated as below:

$$
\begin{bmatrix} [K_{dd}] & [K_{db}] \\ [K_{bd}] & [K_{bb}] \end{bmatrix} \begin{Bmatrix} \{\lambda_d\} \\ \{\lambda_b\} \end{Bmatrix} = \omega^2 \begin{bmatrix} [M_{dd}] & [M_{db}] \\ [M_{bd}] & [M_{bb}] \end{bmatrix} \begin{Bmatrix} \{\lambda_d\} \\ \{\lambda_b\} \end{Bmatrix} \tag{24}
$$

where the indices 'b' and 'd' correspond to the border and domain, respectively, and 'λ' is the mode shape (Ebrahimi and Shafiei 2017, Ebrahimi *et al*. 2017, Ehyaei *et al*. 2017b, Ghadiri *et al*. 2017a, b, c, d, e, Mirjavadi *et al*. 2017a, b, c, d, Shafiei *et al*. 2017a, b, c, d, 2019, 2020, Shafiei and Kazemi 2017a, Shivanian *et al*. 2017, Azimi *et al*. 2018, Shafiei and She 2018).

5. Results and discussions

Before the discussion of the results, the following nondimensional parameters should be define:

$$\mu_{e_0a} = \frac{e_0 a}{R_0} \tag{25a}$$

$$\mu_l = \frac{l}{R_0} \tag{25b}$$

$$\Psi = \omega \frac{L^2}{R_0}\sqrt{\frac{\rho_0}{E_0}} \tag{25c}$$

where μ_{e_0a} , μ_l and Ψ are non-dimensional nonlocal parameter, non-dimensional gradient parameter and non-dimensional frequency. R_O is outer radius of tube and $E_0 = 201.04$ GPa, $\rho_0 = 8166 \frac{\text{Kg}}{m^3}$. To prove the correctness of the present study, the first two natural dimensionless frequency parameters Ψ for simply supported (S-S) Al_2O_3/Nickel nanotubes are given in Table 2. From Table 2, we can see that the present results are consistent with the existing results, thus, the correctness of the present study is confirmed.

Table 2 Comparisons of natural frequency parameter for Si_3N_4/SUS304 nanotubes (S-S) ($n = 1, R_i/R_0 = 0.5,\ \Delta T = 0,\ L/h = 20,\ \beta = 0$)

		First frequency, - $(\Psi_1)^2$	Second frequency, $(\Psi_2)^2$
$\mu_{e0a} = \mu_l = 0$	(Shafiei and She 2018) (Navier solution method)	67.79876	970.5717
	Present (GDQM)	67.77202	968.1735
$\mu_{e0a} = 1$, $\mu_l = 0$	(Shafiei and She 2018) (Navier solution method)	66.16196	883.3973
	Present (GDQM)	66.14008	883.3832
$\mu_{e0a} = 3$, $\mu_l = 0$	(Shafiei and She 2018) (Navier solution method)	55.4876	514.0196
	Present (GDQM)	55.4936	514.0216
$\mu_{e0a} = 0$, $\mu_l = 1$	(Shafiei and She 2018) (Navier solution method)	69.47223	1066.349
	Present (GDQM)	69.70663	1066.385
$\mu_{e0a} = 0$, $\mu_l = 3$	(Shafiei and She 2018) (Navier solution method)	82.86461	1832.696
	Present (GDQM)	82.84754	1832.736

For Al_2O_3/Nickel FG nanotubes with varied boundary conditions, the first two natural dimensionless frequency (Ψ^2) are reported in Tables 3-5. According to Tables 3-5, the current high-order findings are marginally inferior to those predicted by the Timoshenko beam model. Furthermore, the frequency grows and lowers depending on the radial and length aspect ratios, as well as the influence of the radial aspect ratio is more significant than that of the radial. For simply-supported and clamped boundary conditions, the fundamental and second frequencies were shown to decrease with a non-dimensional nonlocal parameter.

The first two natural frequencies of Al_2O_3/Nickel nano-scaled tubes with different boundary conditions against the dimensionless nonlocal parameter μ_{e_0a} are shown in Figs. 2 and 3, respectively for higher-order theory result. As can be seen, for any supported ends, the frequency decreases with the increase in nonlocal parameter μ_{e_0a} and the power law index "n", that is due to the fact that, as power law index "n" or nonlocal parameter μ_{e_0a} rise, the stiffness of the tubes decreases, correspondingly, the vibration frequency decreases. So, it is obvious that the nonlocal cantilever nano-scaled tube can capture the stiffness softening characteristics by nonlocal boundary conditions. Many researchers present this fact, the frequency of the cantilever tube or beam (clamped-free boundary condition) increases with nonlocal parameter (Aranda-Ruiz *et al*. 2012), it can be true for when the free boundary condition was as local (it means this boundary was independent to time and nonlocal parameter), but, by using the nonlocal boundary conditions in free edge, it can see the frequency of cantilever decreases with the nonlocal parameter.

The first two natural frequencies of Al_2O_3/Nickel nano-scaled tubes with different boundary conditions against the dimensionless nonlocal parameter μ_{e_0a} are shown in Figs. 2 and 3, respectively for higher-order theory result. As can

Table 3 Comparisons of natural frequency (Ψ^2) parameter for Al_2O_3/Nickel nanotubes (R_o = 20 R_i = L/40 = 1 (nm), μ_l = 1, n = 1, ΔT = 10K)

		First frequency		Second frequency	
		Timoshenko (g = z)	**Higher order**	Timoshenko (g = z)	**Higher order**
SS	μ_{e0a} = 0	63.05646	62.9963	1060.862	1057.099
	μ_{e0a} = 1	62.64447	62.58467	1034.919	1031.246
	μ_{e0a} = 2	61.43825	61.37954	964.0807	960.6552
	μ_{e0a} = 3	59.52188	59.46488	865.0869	862.0072
	μ_{e0a} = 4	57.01971	56.96495	755.9161	753.2176
	μ_{e0a} = 5	54.07773	54.0256	649.8257	647.4978
	μ_{e0a} = 6	50.84497	50.79573	554.0467	552.0533
CS	μ_{e0a} = 0	158.1237	157.3617	1687.67	1670.116
	μ_{e0a} = 1	156.94	156.1871	1643.553	1626.679
	μ_{e0a} = 2	153.4859	152.7592	1523.82	1508.722
	μ_{e0a} = 3	148.0335	147.347	1358.308	1345.508
	μ_{e0a} = 4	140.9797	140.3433	1178.277	1167.774
	μ_{e0a} = 5	132.7806	132.1999	1005.882	997.3855
	μ_{e0a} = 6	123.8893	123.3659	852.4283	845.5671
CC	μ_{e0a} = 0	334.9041	331.6092	2542.204	2495.426
	μ_{e0a} = 1	332.2732	329.0242	2472.247	2427.521
	μ_{e0a} = 2	324.6051	321.4879	2283.043	2243.626
	μ_{e0a} = 3	312.5291	309.613	2023.196	1990.504
	μ_{e0a} = 4	296.9584	294.2902	1742.987	1716.83
	μ_{e0a} = 5	278.9357	276.5386	1477.27	1456.644
	μ_{e0a} = 6	259.4863	257.3632	1243.108	1226.838

Table 4 Comparisons of natural frequency (Ψ^2) parameter for Al_2O_3/Nickel nanotubes (R_o = 20 R_i = L/100 = 1 (nm), μ_l = 1, n = 1, ΔT = 10K)

		First frequency		Second frequency	
		Timoshenko (g = z)	**Higher order**	Timoshenko (g = z)	**Higher order**
SS	μ_{e0a} = 0	41.21884	41.22853	970.6741	971.2919
	μ_{e0a} = 1	41.16231	41.15263	967.0647	966.4494
	μ_{e0a} = 2	40.95477	40.96442	953.9723	954.5805
	μ_{e0a} = 3	40.62758	40.63719	933.8113	934.408
	μ_{e0a} = 4	40.17486	40.1844	906.8438	907.4249
	μ_{e0a} = 5	39.60176	39.61122	874.1645	874.7268
	μ_{e0a} = 6	38.91466	38.92402	836.9844	837.5254
CS	μ_{e0a} = 0	133.4227	133.3113	1606.222	1603.39
	μ_{e0a} = 1	133.206	133.0948	1598.722	1595.909
	μ_{e0a} = 2	132.5589	132.4484	1576.599	1573.841
	μ_{e0a} = 3	131.4901	131.3808	1540.942	1538.271
	μ_{e0a} = 4	130.0139	129.9062	1493.419	1490.862
	μ_{e0a} = 5	128.1498	128.0441	1436.096	1433.674
	μ_{e0a} = 6	125.9214	125.818	1371.232	1368.957
CC	μ_{e0a} = 0	311.9977	311.489	2491.952	2484.183
	μ_{e0a} = 1	311.4828	310.9754	2479.576	2471.867
	μ_{e0a} = 2	309.9453	309.4418	2443.106	2435.574
	μ_{e0a} = 3	307.4074	306.9103	2384.434	2377.18
	μ_{e0a} = 4	303.9049	303.4165	2306.448	2299.555
	μ_{e0a} = 5	299.4863	299.0088	2212.704	2206.232
	μ_{e0a} = 6	294.2111	293.7464	2107.06	2101.045

Table 5 Comparisons of natural frequency (Ψ^2) parameter for Al_2O_3/Nickel nanotubes (R_o = 50 R_i = L/40 = 1 (nm), μ_l = 1, n = 1, ΔT = 10K)

		First frequency		Second frequency	
		Timoshenko (g = z)	**Higher order**	Timoshenko (g = z)	**Higher order**
SS	μ_{e0a} = 0	63.87944	63.82108	1074.596	1070.944
	μ_{e0a} = 1	63.46215	63.40415	1048.318	1044.754
	μ_{e0a} = 2	62.24043	62.18347	976.5658	973.2419
	μ_{e0a} = 3	60.29942	60.24412	876.2951	873.3068
	μ_{e0a} = 4	57.76508	57.71196	765.7162	763.0978
	μ_{e0a} = 5	54.78528	54.73471	658.2574	655.9985
	μ_{e0a} = 6	51.51096	51.4632	561.243	559.3087
CS	μ_{e0a} = 0	160.1749	159.4146	1709.568	1692.132
	μ_{e0a} = 1	158.976	158.2248	1664.88	1648.124
	μ_{e0a} = 2	155.4776	154.7527	1543.596	1528.617
	μ_{e0a} = 3	149.9553	149.2708	1375.942	1363.258
	μ_{e0a} = 4	142.8111	142.1769	1193.582	1183.189
	μ_{e0a} = 5	134.5069	133.9287	1018.956	1010.563
	μ_{e0a} = 6	125.5016	124.9808	863.5182	856.7508
CC	μ_{e0a} = 0	339.2438	335.943	2575.299	2528.579
	μ_{e0a} = 1	336.5791	333.3246	2504.431	2459.775
	μ_{e0a} = 2	328.8127	325.6911	2312.766	2273.446
	μ_{e0a} = 3	316.5817	313.6629	2049.54	2016.973
	μ_{e0a} = 4	300.8113	298.1424	1765.691	1739.676
	μ_{e0a} = 5	282.5575	280.1617	1496.524	1476.045
	μ_{e0a} = 6	262.8587	260.7387	1259.323	1243.197

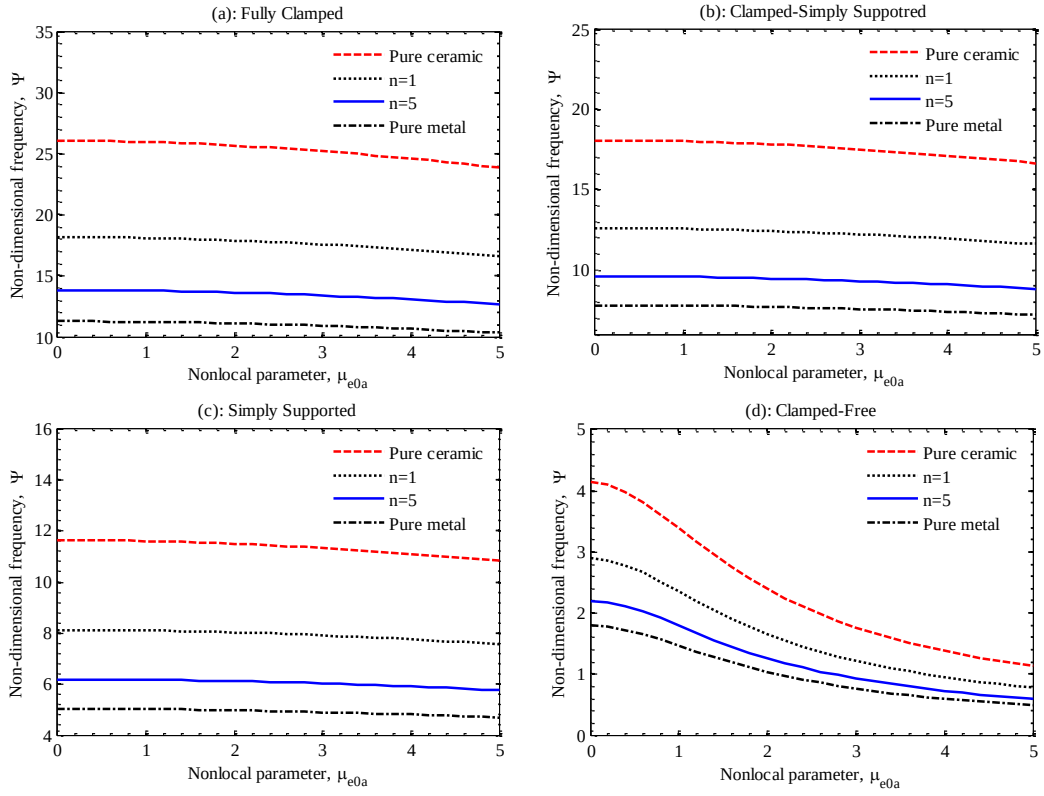

Fig. 2 The variation of the first-order frequency against nonlocal parameter μ_{e_0a} for the Al_2O_3/Nickel nano-scaled tubes with different boundary conditions and power law index (R_o = 10 R_i = L/40 = 1 (nm), β = 0, μ_l = 0)

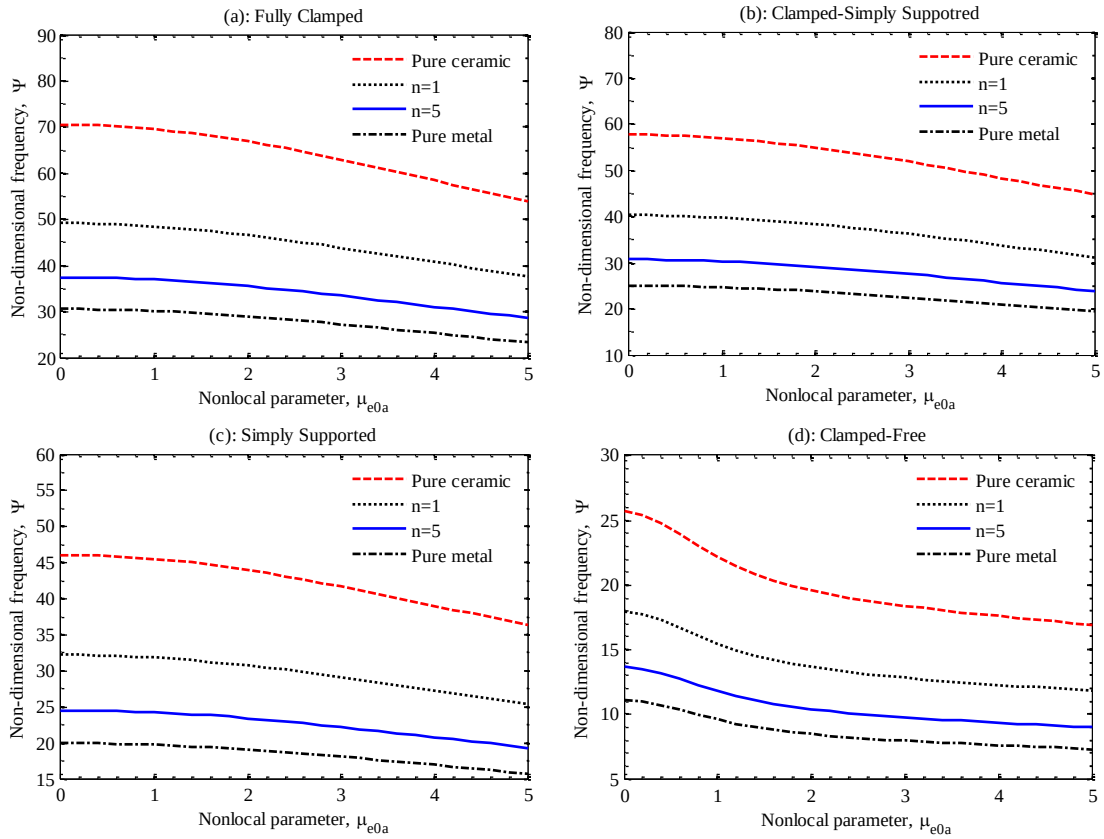

Fig. 3 The variation of the second-order frequency against nonlocal parameter μ_{e_0a} for the Al_2O_3/Nickel nano-scaled tubes with different boundary conditions and power law index (R_o = 10 R_i = L/40 = 1 (nm), β = 0, μ_l = 0)

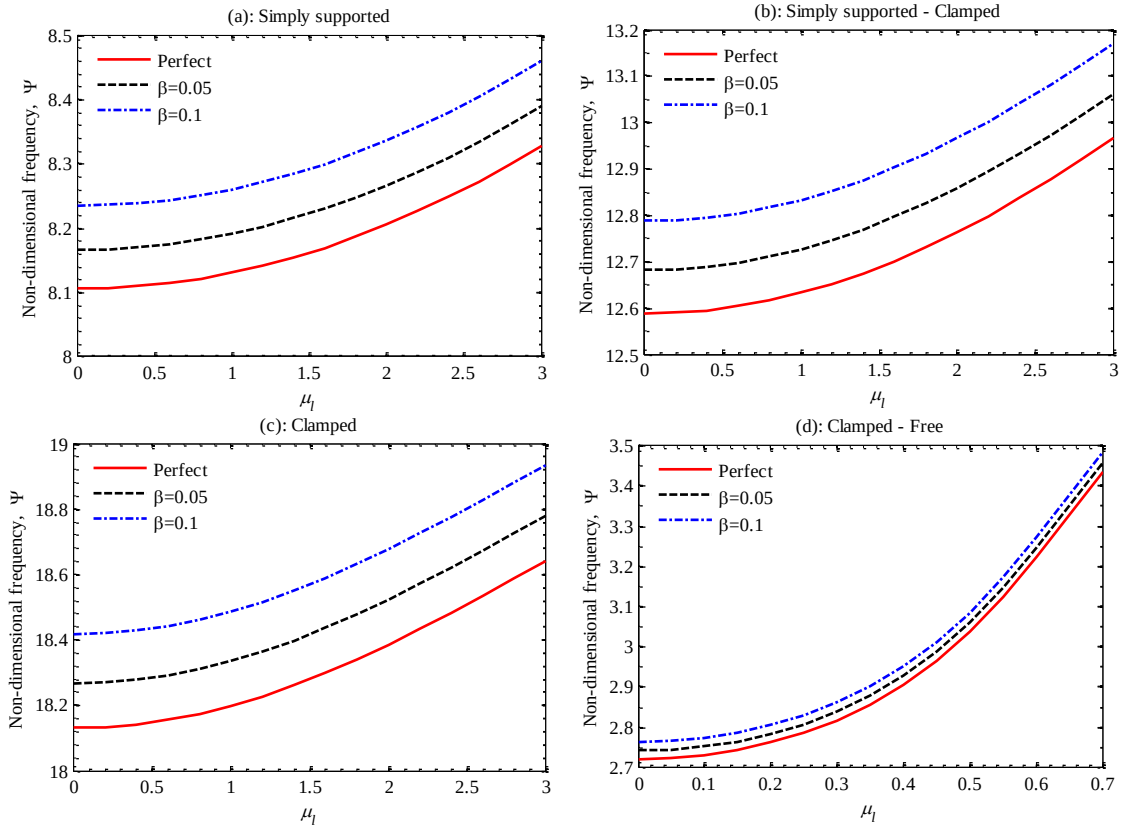

Fig. 4 The variation of the first-order frequency against the porosity volume fraction β for the Al_2O_3/Nickel nanotubes with different boundary conditions and strain gradient parameter μ_l (n = 1, R_o = 10 R_i = L/40 = 1 (nm), μ_{ea} = 0.5)

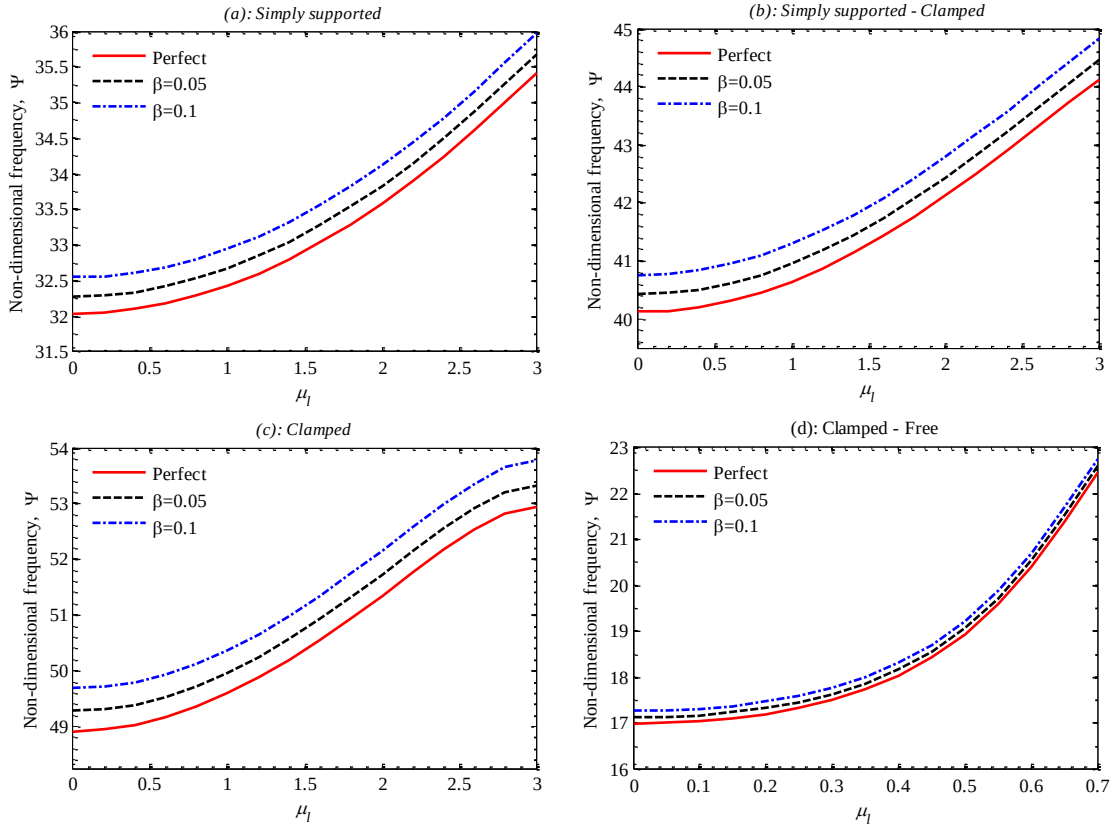

Fig. 5 The variation of the second-order frequency against the porosity volume fraction β for the Al_2O_3/Nickel nanotubes with different boundary conditions and strain gradient parameter μ_l (n = 1, R_o = 10 R_i = L/40 = 1 (nm), μ_{ea} = 0.5)

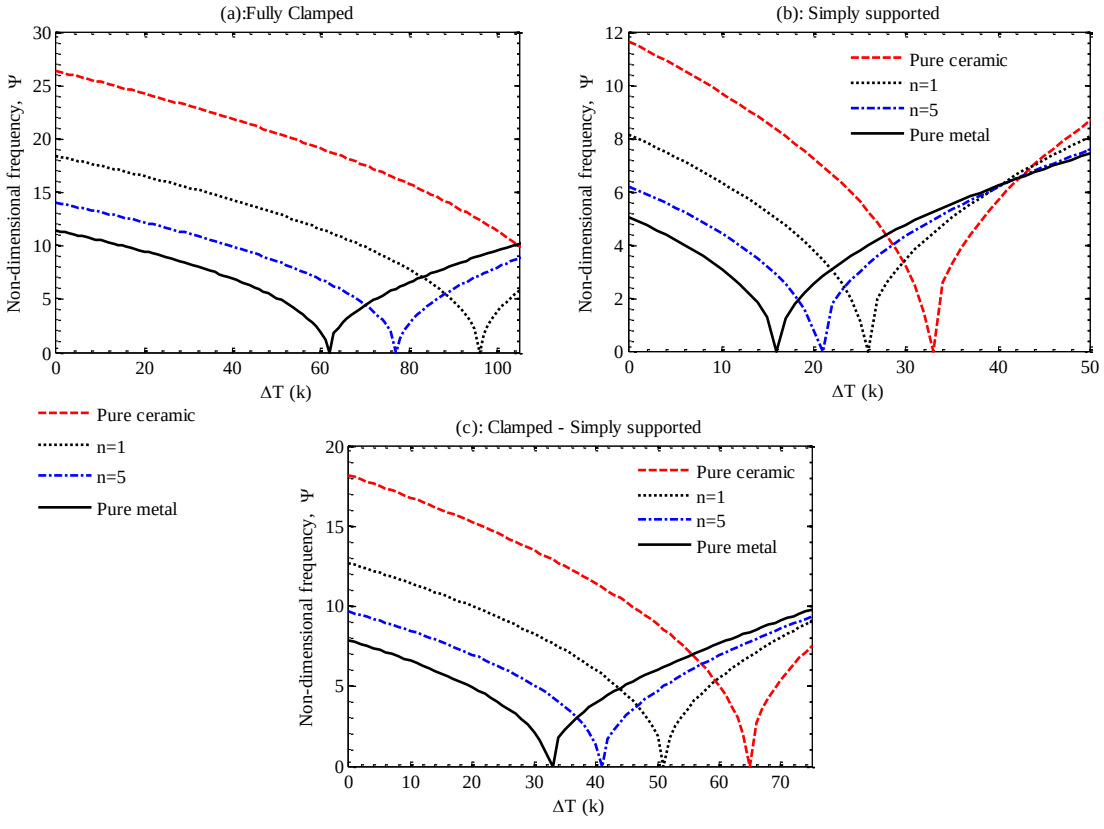

Fig. 6 The variation of the fundamental frequency nanotubes versus temperature change in various FG power index parameter, R_o = 10 R_i = L/100 = 1 (nm), μ_{e0a} = μ_l = 2

Table 6 Effect on temperature on the first two frequency (Ψ^2) for the Al_2O_3/Nickel nanotubes with clamped-clamped ends ($\beta = 0.05$, n = 1, R_o = 1nm, L = $10R_o$)

	T(K)	Fundamental frequency			Second frequency		
		$R_o = 2R_i$	$R_o = 4R_i$	$R_o = 8R_i$	$R_o = 2R_i$	$R_o = 4R_i$	$R_o = 8R_i$
$\mu_{e0a} = 0.5$ $\mu_l = 0$	ΔT = 0	212.1573	212.913	220.2716	990.0569	1055.203	212.1573
	ΔT = 10	211.5323	212.2665	219.5959	987.4294	1052.369	211.5323
	ΔT = 20	210.901	211.6152	218.9169	984.7709	1049.511	210.901
	ΔT = 40	209.6194	210.2987	217.5478	979.3639	1043.72	209.6194
	ΔT = 80	206.9789	207.6098	214.7646	968.1799	1031.835	206.9789
$\mu_{e0a} = 0$ $\mu_l = 0.5$	ΔT = 0	224.9979	224.0311	231.3055	1217.005	1265.577	224.9979
	ΔT = 10	224.3776	223.3907	230.6365	1214.079	1262.456	224.3776
	ΔT = 20	223.751	222.7458	229.9639	1211.117	1259.308	223.751
	ΔT = 40	222.4787	221.443	228.6084	1205.086	1252.928	222.4787
	ΔT = 80	219.8562	218.7817	225.8543	1192.584	1239.828	219.8562
$\mu_{e0a} = 0.5$ $\mu_l = 0.5$	ΔT = 0	219.1371	218.3328	225.4682	1109.284	1154.243	219.1371
	ΔT = 10	218.5146	217.6888	224.7951	1106.505	1151.276	218.5146
	ΔT = 20	217.8856	217.0404	224.1189	1103.693	1148.283	217.8856
	ΔT = 40	216.6089	215.73	222.7553	1097.965	1142.219	216.6089
	ΔT = 80	213.9769	213.0531	219.9841	1086.099	1129.767	213.9769

be seen, for any supported ends, the frequency decreases with the increase in nonlocal parameter $\mu_{e_0 a}$ and the power law index "n", that is due to the fact that, as power law index "n" or nonlocal parameter $\mu_{e_0 a}$ rise, the stiffness of the tubes decreases, correspondingly, the vibration frequency decreases. So, it is obvious that the nonlocal cantilever nano-scaled tube can capture the stiffness softening characteristics by nonlocal boundary conditions. Many researchers present this fact, the frequency of the cantilever tube or beam (clamped-free boundary condition) increases with nonlocal parameter (Aranda-Ruiz *et al*. 2012), it can be true for when the free boundary condition was as local (it means this boundary was independent to time and nonlocal parameter), but, by using the nonlocal boundary conditions in free edge, it can see the frequency of cantilever decreases with the nonlocal parameter.

The influence of temperature on the vibration frequency is given in Table 6, and as can be seen from the table, the rise in temperature and aspect ratio in radial direction causes a decrease and increase in frequency, respectively, Because of this fact, increases in the stiffness cause the frequency rise, and it's clearly shown the stiffness of the tube increases with aspect ratio in the radial direction (R_o/R_i) and decreases with ΔT. Moreover, the decrease in frequency because of the size effect is more in the nonlocal parameter, in fact, the decrease of frequency because of the gradient strain parameter is smaller than the nonlocal one.

Fig. 6 shows the first frequency of FG nanotubes with fully clamped, simply supported and clamped-simply supported boundary conditions for various temperature change (ΔT) and FG power index (n). It can be seen from Fig. 6 that the effect of temperature variations on natural frequencies of the tubes is not a monotonic function, and the temperature-frequency curves of Fig. 6 indicate that, the frequency lowers within a particular range as the temperature rises, until it touches zero, and then rises again if the temperature is high enough. The frequency before thermal buckling reduces when the FG power index (n) is increased. Temperature change, on the other hand, reduces frequency before buckling, then raises frequency as ΔT rises. The emergence of temperature buckling is also postponed by reductions in FG power index owing to increased stiffness of nanotubes.

6. Conclusions

The free vibration of FG nano-scaled tubes is investigated in this study. The governing equations are constructed and solved using the extended differential quadrature technique, using nonlocal strain gradient theory to capture the small size effects. The numerical examples demonstrate how varied boundary conditions, a tiny size parameter, temperature fluctuations, porosity volume fractions, and the power-law index affect the natural frequencies of porous tubes. The frequency of the porous tubes reduces as the temperature, porosity volume fraction, and power-law index increase. The current research also reveals that the stiffness softening properties of tubes with clamped-free ends may be captured by their fundamental frequency. Briefly,

- As stiffness increases, the frequency rises.
- Because stiffness decreases, the nonlocal and gradient strain parameters reduce frequency.
- The contribution of the nonlocal parameter is more significant than that of the gradient strain parameter, indicating that the nonlocal parameter reduces stiffness more than the gradient strain.
- In the radius direction, the aspect ratio improves stiffness.

• The frequency is increased by increasing the porosity parameter.

• When the nonlocal parameter is used with the local parameter of the boundary condition, the frequency increases.

• With the nonlocal parameter, the nonlocal boundary condition for the free end tube causes the frequency to drop.

• Using the nonlocal parameter, the frequency of wholly clamped, simply supported, and clamped-simply supported boundary conditions is reduced.

• For all boundary conditions, the frequency rises when the gradient strain parameter increases.

References

Aifantis, E.C. (1992), "On the role of gradients in the localization of deformation and fracture", *Int. J. Eng. Sci.*, **30**(10), 1279-1299. https://doi.org/10.1016/0020-7225(92)90141-3.

Akbaş, S.D. (2018a), "Forced vibration analysis of cracked functionally graded microbeams", *Adv. Nano Res.*, **6**(1), 39-55. http://doi.org/10.12989/anr.2018.6.1.039.

Akbaş, Ş.D. (2018b), "Bending of a cracked functionally graded nanobeam", *Adv. Nano Res.*, **6**(3), 219-242. http://doi.org/10.12989/anr.2018.6.3.219.

Alipour, M., Torabi, M.A., Sareban, M., Lashini, H., Sadeghi, E., Fazaeli, A., Habibi, M. and Hashemi, R. (2020), "Finite element and experimental method for analyzing the effects of martensite morphologies on the formability of DP steels", *Mech. Based Des. Struct.*, **48**(5), 525-541. http://doi.org/10.1080/15397734.2019.1633343.

Allahkarami, F., Nikkhah-Bahrami, M. and Saryazdi, M.G. (2017), "Damping and vibration analysis of viscoelastic curved microbeam reinforced with FG-CNTs resting on viscoelastic medium using strain gradient theory and DQM", *Steel Compos. Struct.*, **25**(2), 141-155. https://doi.org/10.12989/scs.2017.25.2.141.

Aranda-Ruiz, J., Loya, J. and Fernández-Sáez, J. (2012), "Bending vibrations of rotating nonuniform nanocantilevers using the Eringen nonlocal elasticity theory", *Compos Struct.*, **94**(9), 2990-3001. https://doi.org/10.1016/j.compstruct.2012.03.033.

Arefi, M. and Zenkour, A.M. (2018), "Free vibration analysis of a three-layered microbeam based on strain gradient theory and three-unknown shear and normal deformation theory", *Steel Compos. Struct.*, **26**(4), 421-437. https://doi.org/10.12989/scs.2018.26.4.421.

Aydogdu, M., Arda, M. and Filiz, S. (2018), "Vibration of axially functionally graded nano rods and beams with a variable nonlocal parameter", *Adv. Nano Res.*, **6**(3), 257-278. http://doi.org/10.12989/anr.2018.6.3.257

Azimi, M., Mirjavadi, S.S., Shafiei, N. and Hamouda, A.M.S. (2016), "Thermo-mechanical vibration of rotating axially functionally graded nonlocal Timoshenko beam", *Appl. Phys. A.*, **123**(1), 104. http://doi.org/110.1007/s00339-016-0712-5.

Azimi, M., Mirjavadi, S.S., Shafiei, N., Hamouda, A.M.S. and Davari, E. (2018), "Vibration of rotating functionally graded Timoshenko nano-beams with nonlinear thermal distribution", *Mech. Adv. Mater. Struct.*, **25**(6), 467-480. http://doi.org/10.1080/15376494.2017.1285455.

Bensaid, I., Bekhadda, A. and Kerboua, B. (2018), "Dynamic analysis of higher order shear-deformable nanobeams resting on elastic foundation based on nonlocal strain gradient theory", *Adv. Nano Res.*, **6**(3), 279-298. http://doi.org/10.12989/anr.2018.6.3.279.

Cheshmeh, E., Karbon, M., Eyvazian, A., Jung, D.w., Habibi, M. and Safarpour, M. (2020), "Buckling and vibration analysis of FG-CNTRC plate subjected to thermo-mechanical load based on higher order shear deformation theory", *Mech. Based Des. Struct.*, 1-24. http://doi.org/10.1080/15397734.2020.1744005.

Dai, Z., Jiang, Z., Zhang, L. and Habibi, M. (2021a), "Frequency characteristics and sensitivity analysis of a size-dependent laminated nanoshell", *Adv. Nano Res.*, **10**(2), 175-189. http://doi.org/10.12989/anr.2021.10.2.175.

Dai, Z., Zhang, L., Bolandi, S.Y. and Habibi, M. (2021b), "On the vibrations of the non-polynomial viscoelastic composite open-type shell under residual stresses", *Compos Struct.*, **263**, 113599. https://doi.org/10.1016/j.compstruct.2021.113599.

Ebrahimi, F., Kokaba, M., Shaghaghi, G. and Selvamani, R. (2020), "Dynamic characteristics of hygro-magneto-thermo-electrical nanobeam with non-ideal boundary conditions", *Adv. Nano Res.*, **8**(2), 169-182. https://doi.org/10.12989/anr.2020.8.2.169.

Ebrahimi, F., Mohammadi, K., Barouti, M.M. and Habibi, M. (2021), "Wave propagation analysis of a spinning porous graphene nanoplatelet-reinforced nanoshell", *Wave. Random Complex*, **31**(6), 1655-1681. https://doi.org/10.1080/17455030.2019.1694729.

Ebrahimi, F. and Shafiei, N. (2016), "Application of Eringen's nonlocal elasticity theory for vibration analysis of rotating functionally graded nanobeams", *Smart Struct. Syst.*, **17**(5), 837-857. https://doi.org/10.12989/sss.2016.17.5.837.

Ebrahimi, F. and Shafiei, N. (2017), "Influence of initial shear stress on the vibration behavior of single-layered graphene sheets embedded in an elastic medium based on Reddy's higher-order shear deformation plate theory", *Mech. Adv. Mater. Struct.*, **24**(9), 761-772. https://doi.org/10.1080/15376494.2016.1196781.

Ebrahimi, F., Shafiei, N., Kazemi, M. and Mousavi Abdollahi, S.M. (2017), "Thermo-mechanical vibration analysis of rotating nonlocal nanoplates applying generalized differential quadrature method", *Mech. Adv. Mater. Struct.*, **24**(15), 1257-1273. https://doi.org/10.1080/15376494.2016.1227499.

Ehyaei, J., Akbarshahi, A. and Shafiei, N. (2017a), "Influence of porosity and axial preload on vibration behavior of rotating FG nanobeam", *Adv. Nano Res.*, **5**(2), 141-169. http://doi.org/10.12989/anr.2017.5.2.141.

Ehyaei, J., Akbarshahi, A. and Shafiei, N. (2017b), "Influence of porosity and axial preload on vibration behavior of rotating FG nanobeam", *Adv. Nano Res.*, **5**(2), 141-169. https://doi.org/10.12989/anr.2017.5.2.141.

Eltaher, M.A., Hamed, M.A., Sadoun, A.M. and Mansour, A. (2014), "Mechanical analysis of higher order gradient nanobeams", *Appl. Math. Comput.*, **229**, 260-272. https://doi.org/10.1016/j.amc.2013.12.076.

Eringen, A.C. (1983), "On differential equations of nonlocal elasticity and solutions of screw dislocation and surface waves", *J. Appl. Phys.*, **54**(9), 4703-4710. https://doi.org/10.1063/1.332803.

Fazaeli, A., Habibi, M. and Ekrami, A.A. (2016), "Experimental and finite element comparison of mechanical properties and formability of dual phase steel and ferrite - pearlite steel with the same chemical composition", *Metall. Eng.*, **19**(2), 84-93. https://doi.org/10.22076/me.2017.41458.1064.

Gafour, Y., Hamidi, A., Benahmed, A., Zidour, M. and Bensattalah, T. (2020), "Porosity-dependent free vibration analysis of FG nanobeam using non-local shear deformation and energy principle", *Adv. Nano Res.*, **8**(1), 37-47. https://doi.org/10.12989/anr.2020.8.1.037.

Ghabussi, A., Habibi, M., NoormohammadiArani, O., Shavalipour, A., Moayedi, H. and Safarpour, H. (2020), "Frequency characteristics of a viscoelastic graphene nanoplatelet–reinforced composite circular microplate", *J. Vib. Control.*, **27**(1-2), 101-118. https://doi.org/10.1177/1077546320923930.

Ghadiri, M. and Shafiei, N. (2016a), "Nonlinear bending vibration of a rotating nanobeam based on nonlocal Eringen's theory using differential quadrature method", *Microsyst. Technol.*, **22**(12), 2853-2867. http://doi.org/10.1007/s00542-015-2662-9.

Ghadiri, M. and Shafiei, N. (2016b), "Vibration analysis of a nano-turbine blade based on Eringen nonlocal elasticity applying the differential quadrature method", *J. Vib. Control*, **23**(19), 3247-3265. http://doi.org/10.1177/1077546315627723.

Ghadiri, M. and Shafiei, N. (2016c), "Vibration analysis of rotating functionally graded Timoshenko microbeam based on modified couple stress theory under different temperature distributions", *Acta Astronautica*, **121**, 221-240. https://doi.org/10.1016/j.actaastro.2016.01.003.

Ghadiri, M., Hosseini, S.H.S. and Shafiei, N. (2016a), "A power series for vibration of a rotating nanobeam with considering thermal effect", *Mech. Adv. Mater. Struct.*, **23**(12), 1414-1420. http://doi.org/10.1080/15376494.2015.1091527.

Ghadiri, M., Shafiei, N. and Akbarshahi, A. (2016b), "Influence of thermal and surface effects on vibration behavior of nonlocal rotating Timoshenko nanobeam", *Appl. Phys. A*, **122**(7), 673. http://doi.org/10.1007/s00339-016-0196-3.

Ghadiri, M., Shafiei, N. and Alireza Mousavi, S. (2016c), "Vibration analysis of a rotating functionally graded tapered microbeam based on the modified couple stress theory by DQEM", *Appl. Phys. A*, **122**(9), 837. http://doi.org/10.1007/s00339-016-0364-5.

Ghadiri, M., Shafiei, N., Salekdeh, S.H., Mottaghi, P. and Mirzaie, T. (2016d), "Investigation of the dental implant geometry effect on stress distribution at dental implant–bone interface", *J. Brazil. Soc. Mech. Sci. Eng.*, **38**(2), 335-343. http://doi.org/10.1007/s40430-015-0472-8.

Ghadiri, M., Mahinzare, M., Shafiei, N. and Ghorbani, K. (2017a), "On size-dependent thermal buckling and free vibration of circular FG Microplates in thermal environments", *Microsyst. Technol.*, **23**(10), 4989-5001. http://doi.org/10.1007/s00542-017-3308-x.

Ghadiri, M., Shafiei, N. and Alavi, H. (2017b), "Thermo-mechanical vibration of orthotropic cantilever and propped cantilever nanoplate using generalized differential quadrature method", *Mech. Adv. Mater. Struct.*, **24**(8), 636-646. http://doi.org/10.1080/15376494.2016.1196770.

Ghadiri, M., Shafiei, N. and Alavi, H. (2017c), "Vibration analysis of a rotating nanoplate using nonlocal elasticity theory", *J. Solid Mech.*, **9**(2), 319-337.

Ghadiri, M., Shafiei, N. and Babaei, R. (2017d), "Vibration of a rotary FG plate with consideration of thermal and Coriolis effects", *Steel Compos. Struct.*, **25**(2), 197-207. http://doi.org/10.12989/scs.2017.25.2.197.

Ghadiri, M., Shafiei, N. and Safarpour, H. (2017e), "Influence of surface effects on vibration behavior of a rotary functionally graded nanobeam based on Eringen's nonlocal elasticity", *Microsyst. Technol.*, **23**(4), 1045-1065. http://doi.org/10.1007/s00542-016-2822-6.

Ghazanfari, A., Assempour, A., Habibi, M. and Hashemi, R. (2016), "Investigation on the effective range of the through thickness shear stress on forming limit diagram using a modified Marciniak–Kuczynski model", **16**(1), 137-143.

Ghazanfari, A., Soleimani, S.S., Keshavarzzadeh, M., Habibi, M., Assempuor, A. and Hashemi, R. (2020), "Prediction of FLD for sheet metal by considering through-thickness shear stresses", *Mech. Based Des. Struct.*, **48**(6), 755-772. http://doi.org/10.1080/15397734.2019.1662310.

Guo, J., Baharvand, A., Tazeddinova, D., Habibi, M., Safarpour, H., Roco-Videla, A. and Selmi, A. (2021a), "An intelligent computer method for vibration responses of the spinning multi-layer symmetric nanosystem using multi-physics modeling", *Eng. Comput.*, 1-22. http://doi.org/10.1007/s00366-021-01433-4.

Guo, Y., Mi, H. and Habibi, M. (2021b), "Electromechanical energy absorption, resonance frequency, and low-velocity impact analysis of the piezoelectric doubly curved system", *Mech. Syst. Signal Pr.*, **157**, 107723. https://doi.org/10.1016/j.ymssp.2021.107723.

Habibi, M., Hashemi, R., Ghazanfari, A., Naghdabadi, R. and Assempour, A. (2016), "Forming limit diagrams by including the M–K model in finite element simulation considering the effect of bending", *Proceedings of the Institution of Mechanical Engineers, Part L: Journal of Materials: Design and Applications*, **232**(8), 625-636. https://doi.org/10.1177/1464420716642258.

Habibi, M., Hashemi, R., Fallah Tafti, M. and Assempour, A. (2018), "Experimental investigation of mechanical properties, formability and forming limit diagrams for tailor-welded blanks produced by friction stir welding", *J. Manuf. Proc.*, **31**, 310-323. https://doi.org/10.1016/j.jmapro.2017.11.009.

Hamidi, A., Houari, M.S.A., Mahmoud, S. and Tounsi, A. (2015), "A sinusoidal plate theory with 5-unknowns and stretching effect for thermomechanical bending of functionally graded sandwich plates", *Steel Compos. Struct.*, **18**(1), 235-253. https://doi.org/10.12989/scs.2015.18.1.235.

Hashemi, H.R., Alizadeh, A.a., Oyarhossein, M.A., Shavalipour, A., Makkiabadi, M. and Habibi, M. (2021), "Influence of imperfection on amplitude and resonance frequency of a reinforcement compositionally graded nanostructure", *Wave. Random Complex*, **31**(6), 1340-1366. https://doi.org/10.1080/17455030.2019.1662968.

He, X., Ding, J., Habibi, M., Safarpour, H. and Safarpour, M. (2021), "Non-polynomial framework for bending responses of the multi-scale hybrid laminated nanocomposite reinforced circular/annular plate", *Thin Wall Struct.*, **166**, 108019. https://doi.org/10.1016/j.tws.2021.108019.

Hosseini, S.M.R., Habibi, M. and Assempour, A. (2018), "Experimental and numerical determination of forming limit diagram of steel-copper two-layer sheet considering the interface between the layers", *Modares Mech. Eng.*, **18**(6), 174-181.

Hou, F., Wu, S., Moradi, Z. and Shafiei, N. (2021), "The computational modeling for the static analysis of axially functionally graded micro-cylindrical imperfect beam applying the computer simulation", *Eng. Comput.*, 1-29. https://doi.org/10.1007/s00366-021-01456-x.

Hu, M., Wang, Y., Yan, Z., Zhao, G., Zhao, Y., Xia, L., Cheng, B., Di, Y. and Zhuang, X. (2021), "Hierarchical dual-nanonet of polymer nanofibers and supramolecular nanofibrils for air filtration with a high filtration efficiency, low air resistance and high moisture permeation", *J. Mater. Chem. A*, **9**(24), 14093-14100. https://doi.org/10.1039/D1TA01505B.

Huang, X., Hao, H., Oslub, K., Habibi, M. and Tounsi, A. (2021a), "Dynamic stability/instability simulation of the rotary size-dependent functionally graded microsystem", *Eng. Comput.*, 1-17. https://doi.org/10.1007/s00366-021-01399-3.

Huang, X., Zhang, Y., Moradi, Z. and Shafiei, N. (2021b), "Computer simulation via a couple of homotopy perturbation methods and the generalized differential quadrature method for nonlinear vibration of functionally graded non-uniform micro-tube", *Eng. Comput.*, 1-18. https://doi.org/10.1007/s00366-021-01395-7.

Huang, X., Zhu, Y., Vafaei, P., Moradi, Z. and Davoudi, M. (2021c), "An iterative simulation algorithm for large oscillation of the applicable 2D-electrical system on a complex nonlinear substrate", *Eng. Comput.*, 1-13. https://doi.org/10.1007/s00366-021-01320-y.

Huo, J., Zhang, G., Ghabussi, A. and Habibi, M. (2021), "Bending analysis of FG-GPLRC axisymmetric circular/annular sector

plates by considering elastic foundation and horizontal friction force using 3D-poroelasticity theory", *Compos Struct*., **276**, 114438. https://doi.org/10.1016/j.compstruct.2021.114438.

Jiao, J., Ghoreishi, S.M., Moradi, Z. and Oslub, K. (2021), "Coupled particle swarm optimization method with genetic algorithm for the static–dynamic performance of the magneto-electro-elastic nanosystem", *Eng. Comput*., 1-15. https://doi.org/10.1007/s00366-021-01391-x.

Li, J., Tang, F. and Habibi, M. (2020a), "Bi-directional thermal buckling and resonance frequency characteristics of a GNP-reinforced composite nanostructure", *Eng. Comput*., 1-22. https://doi.org/10.1007/s00366-020-01110-y.

Li, Y., Li, S., Guo, K., Fang, X. and Habibi, M. (2020b), "On the modeling of bending responses of graphene-reinforced higher order annular plate via two-dimensional continuum mechanics approach", *Eng. Comput*., 1-22. https://doi.org/10.1007/s00366-020-01166-w.

Lim, C.W., Zhang, G. and Reddy, J.N. (2015), "A higher-order nonlocal elasticity and strain gradient theory and its applications in wave propagation", *J. Mech. Phys. Solid.*, **78**, 298-313. https://doi.org/10.1016/j.jmps.2015.02.001.

Liu, Z., Su, S., Xi, D. and Habibi, M. (2020a), "Vibrational responses of a MHC viscoelastic thick annular plate in thermal environment using GDQ method", *Mech. Based Des. Struct*., 1-26. https://doi.org/10.1080/15397734.2020.1784201.

Liu, Z., Wu, X., Yu, M. and Habibi, M. (2020b), "Large-amplitude dynamical behavior of multilayer graphene platelets reinforced nanocomposite annular plate under thermo-mechanical loadings", *Mech. Based Des. Struct*., 1-25. https://doi.org/10.1080/15397734.2020.1815544.

Liu, H., Shen, S., Oslub, K., Habibi, M. and Safarpour, H. (2021a), "Amplitude motion and frequency simulation of a composite viscoelastic microsystem within modified couple stress elasticity", *Eng. Comput.*, 1-25. https://doi.org/10.1007/s00366-021-01316-8.

Liu, H., Zhao, Y., Pishbin, M., Habibi, M., Bashir, M.O. and Issakhov, A. (2021b), "A comprehensive mathematical simulation of the composite size-dependent rotary 3D microsystem via two-dimensional generalized differential quadrature method", *Eng. Comput*., 1-26. https://doi.org/10.1007/s00366-021-01419-2.

Liu, Y., Wang, W., He, T., Moradi, Z. and Larco Benítez, M.A. (2021c), "On the modelling of the vibration behaviors via discrete singular convolution method for a high-order sector annular system", *Eng. Comput*., 1-23. https://doi.org/10.1007/s00366-021-01454-z.

Ma, L., Liu, X. and Moradi, Z. (2021), "On the chaotic behavior of graphene-reinforced annular systems under harmonic excitation", *Eng. Comput.*, 1-25. https://doi.org/10.1007/s00366-020-01210-9.

Matouk, H., Bousahla, A.A., Heireche, H., Bourada, F., Bedia, E., Tounsi, A., Mahmoud, S., Tounsi, A. and Benrahou, K. (2020), "Investigation on hygro-thermal vibration of P-FG and symmetric S-FG nanobeam using integral Timoshenko beam theory", *Adv. Nano Res*., **8**(4), 293-305. https://doi.org/10.12989/anr.2020.8.4.293.

Mindlin, R.D. (1965), "Second gradient of strain and surface-tension in linear elasticity", *Int. J. Solid Struct*., **1**(4), 417-438. https://doi.org/10.1016/0020-7683(65)90006-5.

Mindlin, R.D. and Eshel, N.N. (1968), "On first strain-gradient theories in linear elasticity", *Int. J. Solid. Struct*., **4**(1), 109-124. https://doi.org/10.1016/0020-7683(68)90036-X.

Mirjavadi, S.S., Afshari, B.M., Shafiei, N., Hamouda, A., Kazemi, M. and Structures, C. (2017a), "Thermal vibration of two-dimensional functionally graded (2D-FG) porous Timoshenko nanobeams", *Steel Compos. Struct*., **25**(4), 415-426. https://doi.org/10.12989/scs.2017.25.4.415.

Mirjavadi, S.S., Matin, A., Shafiei, N., Rabby, S. and Mohasel Afshari, B. (2017b), "Thermal buckling behavior of two-dimensional imperfect functionally graded microscale-tapered porous beam", *J. Therm. Stress*., **40**(10), 1201-1214. https://doi.org/10.1080/01495739.2017.1332962.

Mirjavadi, S.S., Mohasel Afshari, B., Shafiei, N., Rabby, S. and Kazemi, M. (2017c), "Effect of temperature and porosity on the vibration behavior of two-dimensional functionally graded micro-scale Timoshenko beam", *J. Vib. Control*., **24**(18), 4211-4225. https://doi.org/10.1177/1077546317721871.

Mirjavadi, S.S., Rabby, S., Shafiei, N., Afshari, B.M. and Kazemi, M. (2017d), "On size-dependent free vibration and thermal buckling of axially functionally graded nanobeams in thermal environment", *Appl. Phys. A.*, **123**(5), 315. https://doi.org/10.1007/s00339-017-0918-1.

Moayedi, H., Aliakbarlou, H., Jebeli, M., Noormohammadiarani, O., Habibi, M., Safarpour, H. and Foong, L.K. (2020a), "Thermal buckling responses of a graphene reinforced composite micropanel structure", **12**(1), 2050010. https://doi.org/10.1142/s1758825120500106.

Moayedi, H., Darabi, R., Ghabussi, A., Habibi, M. and Foong, L.K. (2020b), "Weld orientation effects on the formability of tailor welded thin steel sheets", *Thin Wall Struct*., **149** 106669. https://doi.org/10.1016/j.tws.2020.106669.

Moayedi, H., Ebrahimi, F., Habibi, M., Safarpour, H. and Foong, L.K. (2020c), "Application of nonlocal strain–stress gradient theory and GDQEM for thermo-vibration responses of a laminated composite nanoshell", *Eng. Comput*., **37**(4), 3359-3374. https://doi.org/10.1007/s00366-020-01002-1.

Moradi, Z., Davoudi, M., Ebrahimi, F. and Ehyaei, A.F. (2021), "Intelligent wave dispersion control of an inhomogeneous micro-shell using a proportional-derivative smart controller", *Wave. Random Complex*, 1-24. https://doi.org/10.1080/17455030.2021.1926572.

Najaafi, N., Jamali, M., Habibi, M., Sadeghi, S., Jung, D.w. and Nabipour, N. (2021), "Dynamic instability responses of the substructure living biological cells in the cytoplasm environment using stress-strain size-dependent theory", *J. Biomol. Struct. Dynam*., **39**(7), 2543-2554. https://doi.org/10.1080/07391102.2020.1751297.

Navi, B.R., Mohammadimehr, M. and Arani, A.G. (2019), "Active control of three-phase CNT/resin/fiber piezoelectric polymeric nanocomposite porous sandwich microbeam based on sinusoidal shear deformation theory", *Steel Compos. Struct*., **32**(6), 753-767. https://doi.org/10.12989/scs.2019.32.6.753.

Oyarhossein, M.A., Alizadeh, A.a., Habibi, M., Makkiabadi, M., Daman, M., Safarpour, H. and Jung, D.W. (2020), "Dynamic response of the nonlocal strain-stress gradient in laminated polymer composites microtubes", *Sci. Rep*., **10**(1), 5616. https://doi.org/10.1038/s41598-020-61855-w.

Peng, D., Chen, S., Darabi, R., Ghabussi, A. and Habibi, M. (2021), "Prediction of the bending and out-of-plane loading effects on formability response of the steel sheets", *Arch. Civil Mech. Eng*., **21**(2), 74. https://doi.org/10.1007/s43452-021-00227-1.

Sadri, M., Younesian, D. and Esmailzadeh, E. (2016), "Nonlinear harmonic vibration and stability analysis of a cantilever beam carrying an intermediate lumped mass", *Nonlinear Dynam*., **84**(3), 1667-1682. https://doi.org/10.1007/s11071-016-2596-5.

Shafiei, N., Kazemi, M. and Ghadiri, M. (2016a), "Comparison of modeling of the rotating tapered axially functionally graded Timoshenko and Euler–Bernoulli microbeams", *Physica E*, **83**, 74-87. https://doi.org/10.1016/j.physe.2016.04.011.

Shafiei, N., Kazemi, M. and Ghadiri, M. (2016b), "Nonlinear vibration behavior of a rotating nanobeam under thermal stress using Eringen's nonlocal elasticity and DQM", *Appl. Phys. A*, **122**(8), 728. https://doi.org/10.1007/s00339-016-0245-y.

Shafiei, N., Kazemi, M. and Ghadiri, M. (2016c), "Nonlinear vibration of axially functionally graded tapered microbeams", *Int. J. Eng. Sci.*, **102**, 12-26. https://doi.org/10.1016/j.ijengsci.2016.02.007.

Shafiei, N., Kazemi, M. and Ghadiri, M. (2016d), "On size-dependent vibration of rotary axially functionally graded microbeam", *Int. J. Eng. Sci.*, **101**, 29-44. https://doi.org/10.1016/j.ijengsci.2015.12.008.

Shafiei, N., Kazemi, M., Safi, M. and Ghadiri, M. (2016e), "Nonlinear vibration of axially functionally graded non-uniform nanobeams", *Int. J. Eng. Sci.*, **106**, 77-94. https://doi.org/10.1016/j.ijengsci.2016.05.009.

Shafiei, N., Mousavi, A. and Ghadiri, M. (2016f), "On size-dependent nonlinear vibration of porous and imperfect functionally graded tapered microbeams", *Int. J. Eng. Sci.*, **106**, 42-56. https://doi.org/10.1016/j.ijengsci.2016.05.007.

Shafiei, N., Mousavi, A. and Ghadiri, M. (2016g), "Vibration behavior of a rotating non-uniform FG microbeam based on the modified couple stress theory and GDQEM", *Compos. Struct.*, **149**, 157-169. https://doi.org/10.1016/j.compstruct.2016.04.024.

Shafiei, N. and Kazemi, M. (2017a), "Buckling analysis on the bi-dimensional functionally graded porous tapered nano-/micro-scale beams", *Aerosp. Sci. Technol.*, **66**, 1-11. https://doi.org/10.1016/j.ast.2017.02.019.

Shafiei, N. and Kazemi, M. (2017b), "Nonlinear buckling of functionally graded nano-/micro-scaled porous beams", *Compos. Struct.*, **178**, 483-492. https://doi.org/10.1016/j.compstruct.2017.07.045.

Shafiei, N., Ghadiri, M., Makvandi, H. and Hosseini, S.A. (2017a), "Vibration analysis of Nano-Rotor's Blade applying Eringen nonlocal elasticity and generalized differential quadrature method", *Appl. Math. Modell.*, **43**, 191-206. https://doi.org/10.1016/j.apm.2016.10.061.

Shafiei, N., Kazemi, M. and Fatahi, L. (2017b), "Transverse vibration of rotary tapered microbeam based on modified couple stress theory and generalized differential quadrature element method", *Mech. Adv. Mater. Struct.*, **24**(3), 240-252. https://doi.org/10.1080/15376494.2015.1128025.

Shafiei, N., Mirjavadi, S.S., Afshari, B.M., Rabby, S. and Hamouda, A.M.S. (2017c), "Nonlinear thermal buckling of axially functionally graded micro and nanobeams", *Compos. Struct.*, **168**, 428-439. https://doi.org/10.1016/j.compstruct.2017.02.048.

Shafiei, N., Mirjavadi, S.S., MohaselAfshari, B., Rabby, S. and Kazemi, M. (2017d), "Vibration of two-dimensional imperfect functionally graded (2D-FG) porous nano-/micro-beams", *Comput. Method Appl. M.*, **322**, 615-632. https://doi.org/10.1016/j.cma.2017.05.007.

Shafiei, N. and She, G.L. (2018), "On vibration of functionally graded nano-tubes in the thermal environment", *Int. J. Eng. Sci.*, **133**, 84-98. https://doi.org/10.1016/j.ijengsci.2018.08.004.

Shafiei, N., Ghadiri, M. and Mahinzare, M. (2019), "Flapwise bending vibration analysis of rotary tapered functionally graded nanobeam in thermal environment", *Mech. Adv. Mater. Struct.*, **26**(2), 139-155. https://doi.org/10.1080/15376494.2017.1365982.

Shafiei, N., Hamisi, M. and Ghadiri, M. (2020), "Vibration analysis of rotary tapered axially functionally graded Timoshenko nanobeam in thermal environment", *J. Solid Mech.*, **12**(1), 16-32.

Shao, Y., Zhao, Y., Gao, J. and Habibi, M. (2021), "Energy absorption of the strengthened viscoelastic multi-curved composite panel under friction force", *Arch. Civil Mech. Eng.*, **21**(4), 141. https://doi.org/10.1007/s43452-021-00279-3.

Shariati, A., Jung, D.W., Mohammad-Sedighi, H., Żur, K.K., Habibi, M. and Safa, M. (2020a), "On the vibrations and stability of moving viscoelastic axially functionally graded nanobeams", *Materials*. **13**(7), 1707. https://doi.org/10.3390/ma13071707.

Shariati, A., Jung, D.W., Mohammad-Sedighi, H., Żur, K.K., Habibi, M. and Safa, M. (2020b), "Stability and dynamics of viscoelastic moving rayleigh beams with an asymmetrical distribution of material parameters", *Symmetry*, **12**(4), 586. https://doi.org/10.3390/sym12040586.

Shariati, A., Habibi, M., Tounsi, A., Safarpour, H. and Safa, M. (2021), "Application of exact continuum size-dependent theory for stability and frequency analysis of a curved cantilevered microtubule by considering viscoelastic properties", *Eng. Comput.*, **37**(4), 3629-3648. https://doi.org/10.1007/s00366-020-01024-9.

She, G.L., Ren, Y.R., Yuan, F.G. and Xiao, W.S. (2018a), "On vibrations of porous nanotubes", *Int. J. Eng. Sci.*, **125**, 23-35. https://doi.org/10.1016/j.ijengsci.2017.12.009.

She, G.L., Yuan, F.G. and Ren, Y.R. (2018b), "On wave propagation of porous nanotubes", *Int. J. Eng. Sci.*, **130**, 62-74. https://doi.org/10.1016/j.ijengsci.2018.05.002.

Shi, X., Li, J. and Habibi, M. (2020), "On the statics and dynamics of an electro-thermo-mechanically porous GPLRC nanoshell conveying fluid flow", *Mech. Based Des. Struct.*, 1-37. https://doi.org/10.1080/15397734.2020.1772088.

Shivanian, E., Ghadiri, M. and Shafiei, N. (2017), "Influence of size effect on flapwise vibration behavior of rotary microbeam and its analysis through spectral meshless radial point interpolation", *Appl. Phys. A*, **123**(5), 329. https://doi.org/10.1007/s00339-017-0955-9.

Touloukian, Y.S. and Ho, C. (1970), "Thermal expansion: Nonmetallic solids", *Thermophys. Properties Matter*, **13**, 247-250.

Wang, T., Wei, X., Wang, J., Huang, T., Peng, H., Song, X., Cabrera, L.V. and Pérez-Jiménez, M.J. (2020a), "A weighted corrective fuzzy reasoning spiking neural P system for fault diagnosis in power systems with variable topologies", *Eng. Appl. Artif. Intel.*, **92**, 103680. https://doi.org/10.1016/j.engappai.2020.103680.

Wang, Z., Yu, S., Xiao, Z. and Habibi, M. (2020b), "Frequency and buckling responses of a high-speed rotating fiber metal laminated cantilevered microdisk", *Mech. Adv. Mater. Struct.*, 1-14. https://doi.org/10.1080/15376494.2020.1824284.

Wang, K., Wang, H. and Li, S. (2022a), "Renewable quantile regression for streaming datasets", *Knowledge Base Syst.*, **235**, 107675. https://doi.org/10.1016/j.knosys.2021.107675.

Wang, Y., Cheng, H., Hu, Q., Liu, L., Jia, L., Gao, S. and Wang, Y. (2022b), "Pore structure heterogeneity of Wufeng-Longmaxi shale, Sichuan Basin, China: Evidence from gas physisorption and multifractal geometries", *J. Petrol. Sci. Eng.*, **208**, 109313. https://doi.org/10.1016/j.petrol.2021.109313.

Wu, J. and Habibi, M. (2021), "Dynamic simulation of the ultra-fast-rotating sandwich cantilever disk via finite element and semi-numerical methods", *Eng. Comput.*, 1-17. https://doi.org/10.1007/s00366-021-01396-6.

Xu, W., Pan, G., Moradi, Z. and Shafiei, N. (2021), "Nonlinear forced vibration analysis of functionally graded non-uniform cylindrical microbeams applying the semi-analytical solution", *Compos Struct.*, **275**, 114395. https://doi.org/10.1016/j.compstruct.2021.114395.

Xu, X.J., Deng, Z.C., Zhang, K. and Xu, W. (2016), "Observations of the softening phenomena in the nonlocal cantilever beams", *Compos Struct.*, **145**, 43-57. https://doi.org/10.1016/j.compstruct.2016.02.073.

Xu, X.J., Wang, X.C., Zheng, M.L. and Ma, Z. (2017), "Bending and buckling of nonlocal strain gradient elastic beams", *Compos. Struct.*, **160**, 366-377. https://doi.org/10.1016/j.compstruct.2016.10.038.

Yu, X., Maalla, A. and Moradi, Z. (2022), "Electroelastic high-

order computational continuum strategy for critical voltage and frequency of piezoelectric NEMS via modified multi-physical couple stress theory", *Mech*. *Syst*. *Signal Pr*., **165**, 108373. https://doi.org/10.1016/j.ymssp.2021.108373.

Zhang, X., Tang, Y., Zhang, F. and Lee, C.S. (2016), "A novel aluminum–graphite dual-ion battery", *Adv*. *Energ*. *Mater*., **6**(11), 1502588. https://doi.org/10.1002/aenm.201502588.

Zhang, L., Chen, Z., Habibi, M., Ghabussi, A. and Alyousef, R. (2021a), "Low-velocity impact, resonance, and frequency responses of FG-GPLRC viscoelastic doubly curved panel", *Compos*. *Struct*., **269**, 114000. https://doi.org/10.1016/j.compstruct.2021.114000.

Zhang, X., Shamsodin, M., Wang, H., NoormohammadiArani, O., Khan, A.M., Habibi, M. and Al-Furjan, M.S.H. (2021b), "Dynamic information of the time-dependent tobullian biomolecular structure using a high-accuracy size-dependent theory", *J*. *Biomol*. *Struct*. *Dynam*., **39**(9), 3128-3143. https://doi.org/10.1080/07391102.2020.1760939.

Zhang, Y., Wang, Z., Tazeddinova, D., Ebrahimi, F., Habibi, M. and Safarpour, H. (2021c), "Enhancing active vibration control performances in a smart rotary sandwich thick nanostructure conveying viscous fluid flow by a PD controller", *Wave*. *Random Complex*, 1-24. https://doi.org/10.1080/17455030.2021.1948627.

Zhao, X., Xia, H., Pan, L., Song, H., Niu, W., Wang, R., Li, R., Bian, X., Guo, Y. and Qin, Y. (2021a), "Drought monitoring over yellow river basin from 2003–2019 using reconstructed MODIS land surface temperature in google earth engine", *Remote Sens*., **13**(18), 3748. https://doi.org/10.3390/rs13183748.

Zhao, Y., Moradi, Z., Davoudi, M. and Zhuang, J. (2021b), "Bending and stress responses of the hybrid axisymmetric system via state-space method and 3D-elasticity theory", *Eng*. *Comput*., 1-23. https://doi.org/10.1007/s00366-020-01242-1.

Zhou, C., Zhao, Y., Zhang, J., Fang, Y. and Habibi, M. (2020), "Vibrational characteristics of multi-phase nanocomposite reinforced circular/annular system", *Adv*. *Nano Res*., **9**(4), 295-307. https://doi.org/10.12989/anr.2020.9.4.295.

JL